International Journal of Heat and Mass Transfer 115 (2017) 73–79

Contents lists available at ScienceDirect

International Journal of Heat and Mass Transfer

journal homepage: www.elsevier.com/locate/ijhmt

Effective thermal conductivity modeling of consolidated sorption composites containing graphite flakes

Khorshid Fayazmanesh, Sina Salari, Majid Bahrami *

Laboratory for Alternative Energy Conversion (LAEC), School of Mechatronic Systems Engineering, Simon Fraser University, 250-13450 102 Avenue, Surrey, BC V3T 0A3, Canada

ARTICLE INFO

Article history:
Received 15 March 2017
Received in revised form 2 July 2017
Accepted 4 July 2017
Available online 14 July 2017

Keywords:
Thermal conductivity
Consolidated composite adsorbent
Silica gel
Natural flake graphite
Thermally conductive additive

ABSTRACT

Thermal conductivity of $CaCl_2$-silica gel composites adsorbent, which is generally used in water-based adsorption cooling systems, can be enhanced by adding natural flakes graphite and consolidating the mixture with a binder. In this study, a bound conduction model with a unit cell approach is employed to predict the effective thermal conductivity of consolidated composite. The model takes the volume fraction, flake size and orientation of the graphite flakes as input, and calculates the effective thermal conductivity of the consolidated mixture. To validate the model result with experimental data, consolidated adsorbents with 0–20 wt% graphite flakes were prepared and their thermal conductivity was measured by Transient Plane Source (TPS) method. The results show that the addition of graphite flakes into consolidated adsorbent increases thermal conductivity from 0.13 to 0.57 $W \cdot m^{-1} \cdot K^{-1}$ when tested at 2% RH and 35 °C. The predictions of the model at steady-state condition qualitatively agreed with the experimental data.

1. Introduction

Heat-driven sorption technology, as a sustainable and clean solution for thermal management and heat storage, has drawn significant interest in academic and industrial research community. This interest has been intensified in the last decade as environmental and climate changes issues are becoming major global challenges. Numerous studies aim to improve material sorption performance, as it is at the core of sorption cooling or storage systems [1]. Due to the nature of sorption process, heat transport properties, e.g. thermal diffusivity and thermal conductivity, of the adsorbent material plays an important role in their performance, since increasing thermal diffusivity can enhance the heat transfer rate that leads to faster sorption/desorption cycles thus more efficient (more compact) heat-driven sorption chillers [2]. A key part of the sorption chillers design is developing adsorbent materials (or composites) with superior hydrophilicity, high water uptake capacity, low regeneration temperature (60–150 °C) [3], and high thermal diffusivity. Silica gel [4] and silicoaluminophosphate [5] have suitable adsorption properties at operating conditions of water-based sorption cooling systems, i.e. low temperature (30–90 °C) and pressure (1.2–5.6 kPa); however, these highly porous sorbents have low effective thermal conductivity 0.13 $W \cdot m^{-1} \cdot K^{-1}$ [6]. Methods used to improve heat transfer in sorption beds include: (i) coating heat exchanger with adsorbent material [2], this will reduce the thermal contact resistance at the interface between the heat exchanger and the coated sorption material; (ii) growing adsorbent on the adsorber bed surface [7]; (iii) adding thermally conductive materials such as metals [8] and consolidating adsorbents in a thermally conductive porous matrix [9], which lead to an increase in the bulk thermal conductivity of sorption composite. The effective thermal conductivity of a wide range of adsorbents reported in the literature is shown in Table 1.

Tanashev et al. [9] measured the thermal conductivity of hygroscopic salts ($CaCl_2$ [10], LiBr and $MgCl_2$) confined silica gel (KSK) with 0.1–0.8 g/g water content using the transient hot wire method at 290–300 K and observed an increase in thermal conductivity from 0.1 to 0.5 $W \cdot m^{-1} \cdot K^{-1}$ with increasing water content. Aristov et al. [11] measured the thermal conductivity of consolidated sorbents, silica gel (KSK) with 36.6 wt% $CaCl_2$ and silica gel (KSK) with 42.7 wt% LiBr and reported that the thermal conductivity increased significantly as the water uptake of the sorbent increased, while the effect of temperature and pressure on thermal conductivity was almost negligible. Restuccia et al. [12] developed and experimentally validated a theoretical model to predict the effective thermal conductivity of wet zeolite. The effective thermal conductivity of zeolite 4A was measured by a hot wire method at different temperatures and water content. All the above-

* Corresponding author.
E-mail address: mbahrami@sfu.ca (M. Bahrami).

http://dx.doi.org/10.1016/j.ijheatmasstransfer.2017.07.020
0017-9310/

Nomenclature

TPS	Transient Plane Source
RH	Relative Humidity
k	thermal conductivity, $W \cdot m^{-1} \cdot K^{-1}$
b	basic cell half side, m
r_p	particle radius, m
r	disk radius, μm
t	disk thickness, μm
w	unit cell width, μm
a	unit cell dimension, μm
R	thermal resistance, $K \cdot W^{-1}$
T	temperature, K
$\dot{Q}$	heat flow rate, W
k_{eff}	effective thermal conductivity, $W \cdot m^{-1} \cdot K^{-1}$
PVP	polyvinylpyrrolidone
t_{sample}	sample thickness, mm
A	sensor area, mm^2
ΔT	temperature rise between sensor and sample, K

Subscripts

e	effective
p	particle
m	medium
L	lower bound
U	upper bound
g	graphite flake
s	continuous medium

Greek symbols

φ	volume fraction
n	shape factor
ψ	sphericity
ρ	density, $g \cdot cm^{-3}$
θ	angle, degree

mentioned studies showed a significant effect of water content on the thermal conductivity of sorption composites.

Fayazmanesh et al. [16] synthesized consolidate composite with addition of copper powder and graphite flakes. Graphite flake particles are distributed evenly in composite adsorbent when copper powder particle inhomogeneously distributed at the bottom surface of samples.

As shown in Table 1, composite adsorbent with expanded graphite has higher thermal conductivity compared to silica or zeolite based composites. This is while the thermal conductivity

Table 1
Thermal conductivity of some adsorbent materials.

Adsorbent	Thermal conductivity, $W \cdot m^{-1} \cdot K^{-1}$	Measurement method and conditions	Ref.
Calcined silica gel (KSK)/$CaCl_2$	0.1–0.5	- Transient hot wire method - Water content (0–0.8 g/g) - Temperature 16–27 °C	[10]
- Consolidated silica gel (KSK)/$CaCl_2$ (36.6 wt%) - Consolidated silica gel (KSK)/LiBr (42.7 wt%)	0.12–0.16 0.1–0.13	- Transient hot wire method - Air pressure: 10–1,000 mbar - Binder: 20 wt% aluminium hydroxide	[11]
Consolidated silica gel (15 wt% binder)	0.24–0.26	- Guarded-hot plate apparatus - Silica gel coated between copper plates - Temperature: 35–50 °C - Contact pressure: 0–90 bar - Polyvinylpyrrolidone used as binder	[6]
- Compressed silica gel (KSK)/$CaCl_2$ - Compressed silica gel (KSK)/LiBr - Compressed silica gel (KSK)/$MgCl_2$ - Alumina/$CaCl_2$	0.12–0.5 0.16–0.4 0.14–0.42 0.12–0.41	- Transient hot wire method - Measurements took place at 16–27 °C - Water content (0–0.9 g/g) - No binder used	[9]
Wetted zeolite 4A	0.17–0.25	- Transient hot wire method - Filling gas: air at 1 bar - Measurement temperatures (50–200 °C) - Water content (0.02–0.2 g/g)	[12]
Consolidated composite activated carbon	1–4	- ASTM E1530 guarded thermal flow meter method - Samples with different ratio of activated carbon were made (33–50%)	[15]
Consolidated silica gel (15 wt% binder)-graphite flake (0–20 wt%)	0.13–0.42	- Transient Plane Source (TPS) - Connected to humidifier - Measurement temperature 35 °C - Relative Humidity 2–20% RH	[16]
Consolidated composite activated carbon	0.9–2.5	- Guarded hot plate method - Samples with different ratio of activated carbon and expanded graphite were made	[17]
- $CaCl_2$ (powder) - $CaCl_2$ (pellet) - Composite-KP50 expanded graphite (20%) and $CaCl_2$ - Consolidated composite- KP50 expanded graphite (20) and $CaCl_2$	0.31–0.39 0.11–0.14 0.4–0.47 0.31–0.47	- Transient hot wire method - Filling gas: air at 1 bar - Measurement take place at different temperature - Different pressure applied for making consolidated samples (0–0.67–20) - Dry samples	[18]

Table 2
Composites prepared with SiliaFlash B60 silica gel matrix.

Sample name	Adsorbent	PVP	Graphite flakes
$CaCl_2$-S6-0%G	4 g, 1.71 g	1 g	–
$CaCl_2$-S6-5%G	4 g, 1.71 g	1 g	0.35 g
$CaCl_2$-S6-10%G	4 g, 1.71 g	1 g	0.74 g
$CaCl_2$-S6-20%G	4 g, 1.71 g	1 g	1.67 g

of silica-/zeolite-based composites are already increased considerably by adding activated carbon.

The objective of this work is to develop a model to predict the effective thermal conductivity of consolidated composite adsorbent containing graphite flakes, considering random orientation of the graphite flakes. Assuming an effective medium theory (applied for thermal conductivity modeling of nano-fluid [13] and catalyst layer in polymer electrolyte membrane fuel cell [14]) and establishing upper and lower bounds, as asymptotes for thermal conductivity, a new model is developed for the effective thermal conductivity of consolidated adsorbent material containing graphite as a function of the volume fraction and orientation of the graphite flakes. Several consolidated samples have been fabricated in our lab and tested to validate the proposed model.

2. Experimental study

2.1. Sample preparation

Silica gel (SiliaFlash® B60, Lot 011112, Silicycle, Inc., Quebec, Canada) with irregular shaped grains (0.2–0.5 mm), average pore diameters of 6 nm and surface area (S_{BET}) 514 $m^2{\cdot}g^{-1}$ was combined with different amount of graphite flakes (Sigma Aldrich, +100 mesh) and 40,000 MW polyvinylpyrrolidone (PVP40, Amresco) binder solution. The slurries were baked for one hour at 50 °C, and then heated to 180 °C for one hour to cross-link the binder. Table 2 shows silica gel composites based adsorbent prepared with different amount of graphite flakes 0–20 wt%.

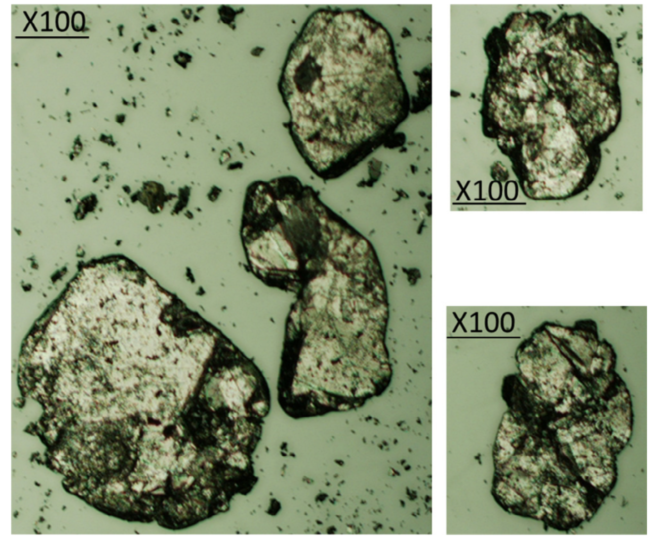

Fig. 2. Optical microscope images of graphite flakes.

2.2. Thermal conductivity measurement

A thermal constants analyzer (TPS 2500S, ThermTest Inc., Fredericton, Canada) capable of precise measurement of thermal conductivity, diffusivity and specific heat was used for this study. The instrument has different sensor types and software modules to perform measurements on bulk materials (isotropic and anisotropic), thin films, powders and liquids. This apparatus uses the transient plane source method in accordance with ISO Standard 22007-2.2. In this study, a bulk sensor (7577) with a 2 mm diameter nickel double spiral insulated in a thin layer of Kapton is used for both transient heating of the sample and temperature measurements. A humidifier (P-10C-1C-2-0-031300-v7, Cellkraft AB, Sweden) is connected to thermal constant analyzer to control the humidity inside the TPS chamber.

For bulk material (isotropic) measurements, the sensor is placed on either side of a pair of dried identical samples. After 20 min for temperature and 2% RH humidity equilibration, measurements are

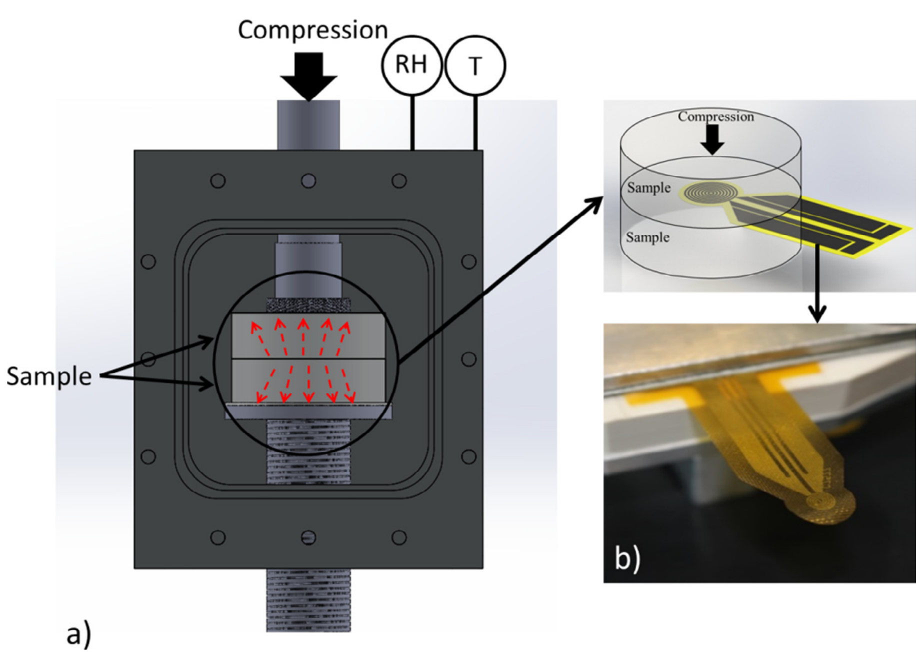

Fig. 1. (a) Sample arrangement schematic in TPS 2500S. (b) Nickel double spiral insulated in a thin layer of Kapton sensor (Sensor 7577).

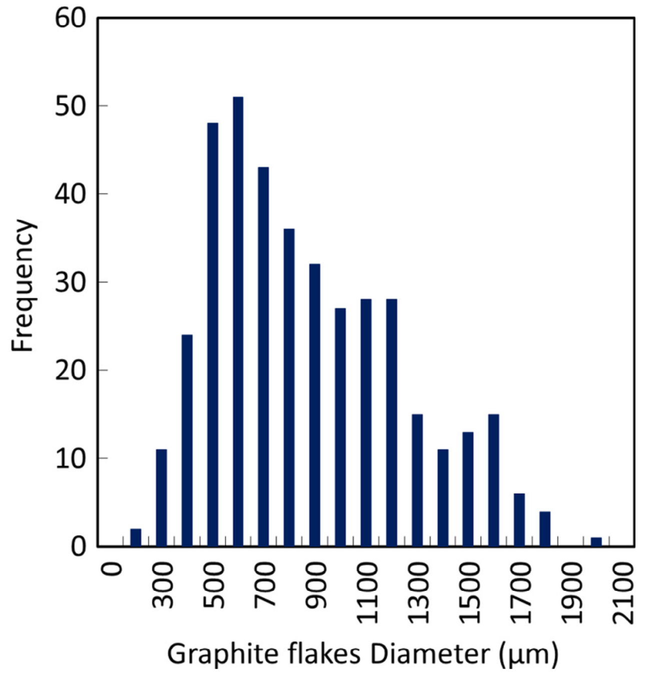

Fig. 3. Graphite flakes diameter measurement distribution of 100 particles.

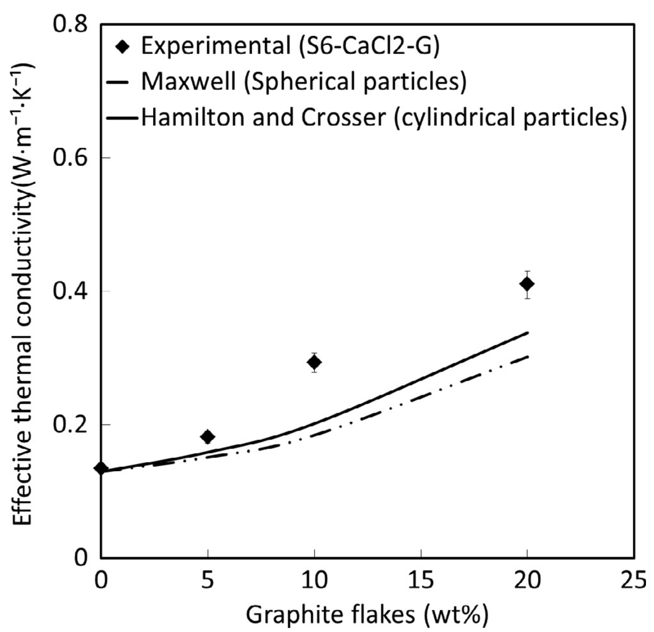

Fig. 4. Comparison of various models with measured thermal conductivity of consolidated composite adsorbents ($CaCl_2$-S6-G) with different amount of graphite flakes (0–20 wt%) at 2% RH.

Table 3
Existing effective thermal conductivity models.

Name	Assumptions	Equation	Ref.
Maxwell's Model	• Dilute dispersion • Spherical particles	$k_e^* = \frac{k_p^*(1+2\phi)+2(1-\phi)}{k_p^*(1-\phi)+(2+\phi)}$ $k_e^* = k_e/k_m$ $k_p^* = k_p/k_m$	[13,19]
Hamilton and Crosser Model	• Spherical and non-spherical particles ($n_{spherical} = 3$, $n_{cylindrical} = 6$)	$k_e^* = \frac{k_p^*[1+(n-1)\phi]+(n-1)(1-\phi)}{k_p^*(1-\phi)+(n-1)+\phi}$ $k_e^* = k_e/k_m$ $k_p^* = k_p/k_m$	[13,19]

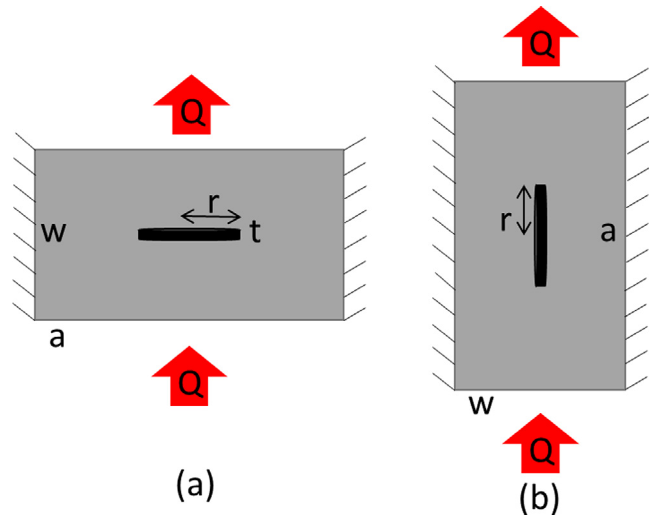

Fig. 5. Disk-shape graphite flakes dispersed in consolidated composite, two extreme cases establishing (a) a lower bound for thermal conductivity (same direction with heat flow) and (b) an upper bound for thermal conductivity (perpendicular to the heat flow direction).

performed on each sample three times at different locations, a standard deviation of 10% has been measured. The sample-sensor assembly is shown in Fig. 1.

Effective thermal conductivity of the sample is calculated by

$$k_{sample} = \frac{\dot{Q}}{A}\frac{t_{sample}}{\Delta T} \tag{1}$$

where $\dot{Q}$ is the power from the heat source, ΔT is the temperature rise between the sensor and sample, A is the sensor area, and t_{sample} is the sample thickness.

2.3. Geometrical parameters of the consolidated graphite-doped composite

Geometrical parameters, i.e. the particle size distribution and graphite flakes size should be measured to be used as input to the model. An optical microscope (Nikon Eclipse LV100) is used to measure the shape and size distribution of 100 graphite flakes, shown in Fig. 2.

Fig. 2 illustrates that the graphite flakes have irregular shapes which make it difficult to use one geometry and one size for geometric modeling. In this study, graphite flakes are assumed to have a disk shape with a diameter, estimated through statistical measurements. The statistical distribution of graphite flakes effective diameter is shown in Fig. 3. The average thickness and diameter for 100 measured graphite flakes is calculated to be 4.3 and 700 μm, with standard deviation of 7%.

3. Model development

Fig. 4 shows a comparison between the existing models in the literature, listed in Table 3, and the present data for thermal conductivity.

As shown in Fig. 4, Maxwell and Hamilton-Crosser models can only predict the thermal conductivity for the sample with 5 wt% and fail to predict higher graphite flake concentrations.

3.1. Bounds of conduction for disk shape particle in basic unit cell

In this section, following the methodology introduced in [13], upper and lower bounds for steady-state through-plane heat conduction in consolidated composite containing graphite flakes

Table 4
Material properties measured at RH = 2%.

$\rho_{silica\ gel}$ (g·cm^{-3})	$\rho_{graphite\ flakes}$ (g·cm^{-3})	$r_{graphite\ falke}$ (μm)	$t_{thicknes}$ (μm)	k_s [measured] (W·m^{-1}·K^{-1})	$k_{g\text{-}in\ plane}$ [20] (W·m^{-1}·K^{-1})	$k_{g\text{-}through\ plane}$ [20] (W·m^{-1}·K^{-1})
0.5	0.64	700	4.3	0.135	750	8

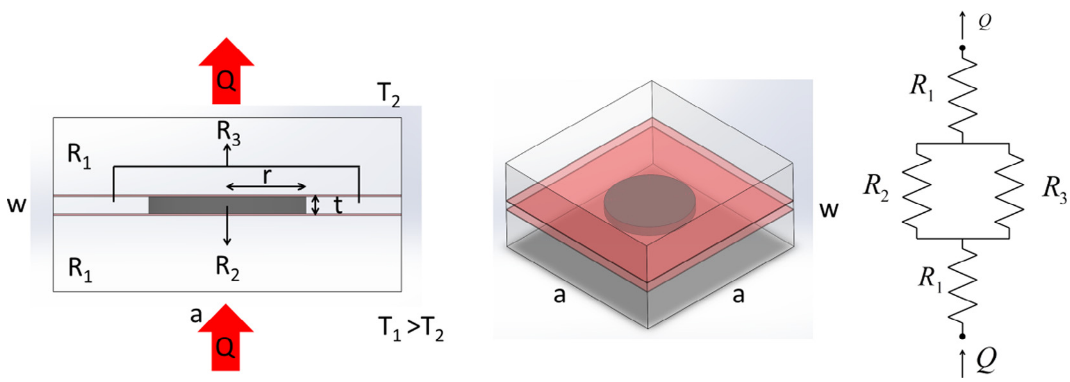

Fig. 6. Lower bound for horizontal disk in unit cell with perpendicular isotherms.

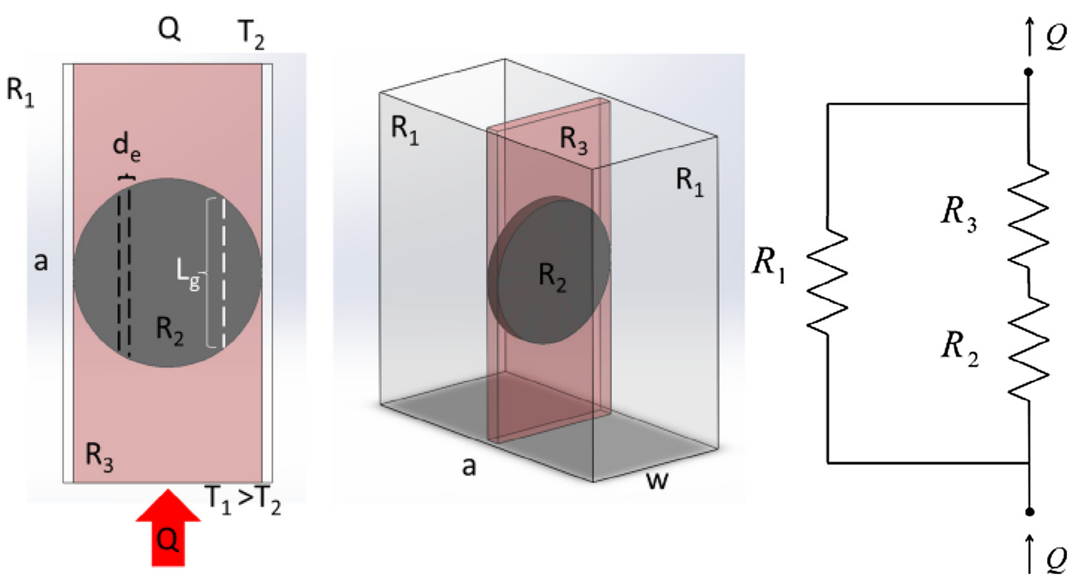

Fig. 7. Upper bound for vertical disk in unit cell with parallel adiabats.

samples are established for horizontally and vertically oriented disk-shaped flakes, as schematically shown in (Fig. 5). A "unit cell" is considered to represent the geometry of the consolidated composite with the dispersed graphite flakes. The size of unit cell depends on the volume fraction of flakes in each sample, and it is calculated using the density of particles and continuous medium. The model is compared to experimental data collected from consolidated composite adsorbent samples, to ensure that the data lays between the upper and lower bound and it is then expanded for particles with a range of orientation angles in a continuous medium.

The assumptions used in development of the present are:

- Identical disk-shape graphite flakes are evenly dispersed throughout the composite.
- The contact between the graphite flakes and the sorption material is perfect, i.e. no thermal contact resistance is considered.
- The sorption material and graphite flakes have constant anisotropic properties, listed in Table 4.

The sorption material in the composite used in this study is $CaCl_2$-silica gel-PVP40.

3.2. Unit cell with disk particles

3.2.1. Lower bound: perpendicular to the heat flow

A lower bound for effective thermal conductivity, and its associated thermal resistance network, can be established by assuming isotherms perpendicular to the direction of heat flow, as shown in Fig. 6.

Based on the thermal resistance network shown in Fig. 6, the lower bound of effective thermal conductivity of the consolidated composite can be found from Eq. (2)

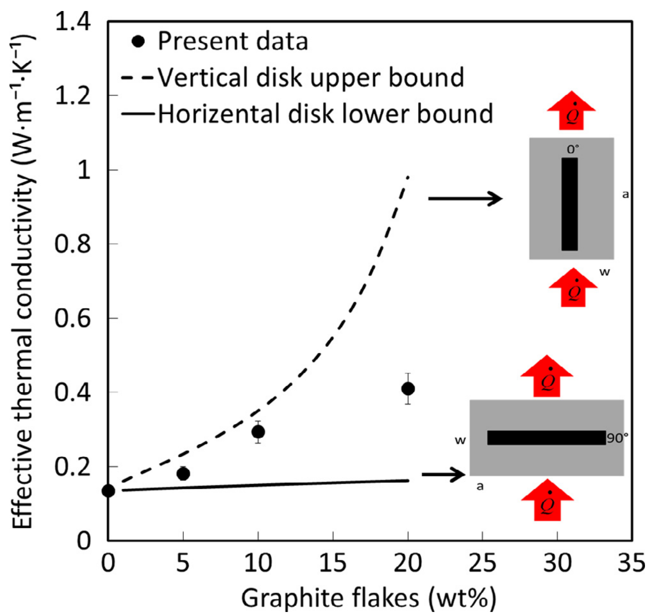

Fig. 8. Highest and lowest possibility of graphite flake orientation in unit cell is shown. Thermal conductivity of consolidated composite adsorbents ($CaCl_2$-S6-G) with different amount of graphite flakes (0–20 wt%) at 2% RH.

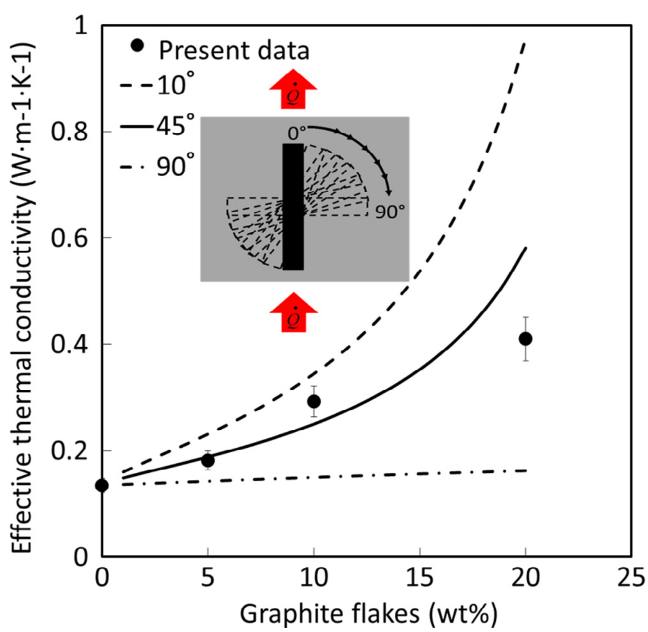

Fig. 9. Thermal conductivity comparison of angled disk particle with uniform distribution in porous medium with measured thermal conductivity of consolidated composite adsorbents ($CaCl_2$-S6-G) with different amount of graphite flakes (0–20 wt%) at 2% RH.

$$k_{eff-L} = \frac{k_s w a^2 \left[k_s(a^2 - \pi r^2) + k_g \pi r^2\right]}{\left[k_s a^2 t + \left[k_s(a^2 - \pi r^2) + k_g \pi r^2\right] \cdot (w - t)\right] \cdot a^2} \tag{2}$$

where w and a are unit cell dimensions.

3.2.2. Upper bound: parallel to heat flow

To calculate the lower bound effective thermal conductivity of a vertical disk particle in a cubic unit cell, parallel adiabats to the direction of heat is assumed, shown in Fig. 7. The similar approach for lower bound calculation used to determine upper bound.

To calculate R_2 and R_3, a new parameter introduced named as L_g,

$$L_g = 2\sqrt{r^2 - d_e^2} \tag{3}$$

Then, the total R_2 and R_3 can be calculated from

$$R_2 = \frac{1}{2t}\int_0^r \left[\frac{a - L_g}{K_s} + \frac{L_g}{K_g}\right] d(d_e) \tag{4}$$

The upper bound effective thermal conductivity can be calculated:

$$k_{eff-U} = \frac{a\int_0^r \left[\frac{a-L_g}{k_s} + \frac{L_g}{k_g}\right] d(d_e)}{w \cdot \left[k_s(wa - 2rt)\int_0^r \left[\frac{a-L_g}{k_s} + \frac{L_g}{k_g}\right] d(d_e) + 2ta\right]} \tag{5}$$

4. Results and discussion

The established upper and lower bounds for effective thermal conductivity of consolidate adsorbent graphite flakes are shown in Fig. 8. As expected the experimental data fall between the two bounds.

In reality, the graphite flakes in the composite adsorbent are expected to be randomly oriented. The introduced upper and lower bounds are used, as two extreme cases, to predict the effective thermal conductivity of the consolidated composites. Using a similar approach, thermal resistance network and effective thermal conductivity can be calculated for consolidated composites containing graphite flake disks with different angles, as shown in Eq. (6):

$$[k_{eff-\theta}] = \cos^2(\theta) \cdot \frac{a\int_0^r \left[\frac{a-L_g}{k_s} + \frac{L_g}{k_g}\right] d(d_e)}{w \cdot \left[k_s(wa - 2rt)\int_0^r \left[\frac{a-L_g}{k_s} + \frac{L_g}{k_g}\right] d(d_e) + 2ta\right]} + \sin^2(\theta) \cdot \frac{k_s w a^2 [K_s(a^2 - \pi r^2) + k_g \pi r^2]}{[k_s a^2 t + [k_s(a^2 - \pi r^2) + k_g \pi r^2] \cdot (w - t)] \cdot a^2} \tag{6}$$

The effective thermal conductivity model of disk particles in different angles compared to the measured thermal conductivity of S6-$CaCl_2$-G, is shown in Fig. 9.

Bound conduction model for disk shaped particles in consolidated sorbent composite shows good agreement with experimental model when the angel of the disk particles is 45°. The relative difference between the experimental data and the modeling result for low volume fraction disk shape thermally conductive additive (0–10 wt%) in continuous medium is 10%. As shown in Fig. 8, graphite flakes have a diameter range of 200–1300 μm which small particles help to make a path through consolidated sorbent composite and improve thermal conductivity.

5. Conclusion

Thermal conductivity of composite adsorbent containing graphite flakes was measured and its effective thermal conductivity with conduction bound method was modeled and measured at 35 °C (2% RH). The results showed thermal conductivity of consolidated composite increased significantly by adding thermally conductive particles.

In addition to the experimental measurements, a new analytical model was developed that can predict the effect of thermally conductive additive on thermal conductivity of consolidated adsorbent. The model captured the trend while different disk shape particles angle and size considered. This model is limited by geometry of additive, volume fraction, the dispersion of particles in composite.

A pressure and temperature jump gravimetric test-bed is built to evaluate the effect of additives on consolidated sorbent performance. Durability of sorbent Coated on graphite sheet with and without additives will be studied.

Conflict of interest

The authors declare that there is no conflict of interest.

Acknowledgment

The authors gratefully acknowledge the financial support of the Natural Sciences and Engineering Research Council of Canada (NSERC) through Automotive Partnership Canada Grant No. APCPJ 429698-1 and Pacific Institute for Climate Solutions (PICS) graduate fellowship.

References

[1] L.G. Gordeeva, Y.I. Aristov, Composites 'salt inside porous matrix' for adsorption heat transformation: a current state-of-the-art and new trends, Int. J. Low-Carbon Technol. 7 (2012) 288–302.
[2] S. Vasta, G. Giacoppo, O. Barbera, L. Calabrese, L. Bonaccorsi, A. Freni, Innovative zeolite coatings on graphite plates for advanced adsorbers, Appl. Therm. Eng. 72 (2014) 153–159.
[3] H. Demir, M. Mobedi, S. Ulku, A review on adsorption heat pump: problems and solutions, Renew. Sustain. Energy Rev. 12 (2008) 2381–2403.
[4] Y.I. Aristov, Challenging offers of material science for adsorption heat transformation: a review, Appl. Therm. Eng. 50 (2) (Feb. 2013) 1610–1618.
[5] A. Freni, L. Bonaccorsi, L. Calabrese, A. Caprì, A. Frazzica, A. Sapienza, SAPO-34 coated adsorbent heat exchanger for adsorption chillers, Appl. Therm. Eng. 82 (2015) 1–7.
[6] A. Sharafian, K. Fayazmanesh, C. McCague, M. Bahrami, Thermal conductivity and contact resistance of mesoporous silica gel adsorbents bound with polyvinylpyrrolidone in contact with a metallic substrate for adsorption cooling system applications, Int. J. Heat Mass Transf. 79 (2014) 64–71.
[7] R.E. Critoph, Y. Zhong, Review of trends in solid sorption refrigeration and heat pumping technology, Proc. Inst. Mech. Eng. Part E J. Process Mech. Eng. 219 (3) (2005) 285–300.
[8] A. Rezk, R.K. Al-Dadah, S. Mahmoud, A. Elsayed, Effects of contact resistance and metal additives in finned-tube adsorbent beds on the performance of silica gel/water adsorption chiller, Appl. Therm. Eng. 53 (2) (2013) 278–284.
[9] Y.Y. Tanashev, A.V. Krainov, Y.I. Aristov, Thermal conductivity of composite sorbents 'salt in porous matrix' for heat storage and transformation, Appl. Therm. Eng. 61 (2) (2013) 401–407.
[10] Y.Y. Tanasheva, Yu. I. Aristov, Thermal conductivity of silica gel + calcium chloride system: the effect of adsorbed water, J. Eng. Phys. Thermophys. 73 (5) (2003) 876–883.
[11] A. Freni, M.M. Tokarev, G. Restuccia, a.G. Okunev, Y.I. Aristov, Thermal conductivity of selective water sorbents under the working conditions of a sorption chiller, Appl. Therm. Eng. 22 (2002) 1631–1642.
[12] B. Dawoud, M.I. Sohel, A. Freni, S. Vasta, G. Restuccia, On the effective thermal conductivity of wetted zeolite under the working conditions of an adsorption chiller, Appl. Therm. Eng. 31 (14–15) (2011) 2241–2246.
[13] M. Bahrami, M.M. Yovanovich, J.R. Culham, Assessment of relevant physical phenomena controlling thermal performance of nanofluids, J. Thermophys. Heat Transf. 21 (4) (2007) 673–680.
[14] S. Salari, C. McCague, M. Tam, M. Saha, J. Stumper, M. Bahrami, Accurate ex-situ measurements of PEM fuel cells catalyst layer dry diffusivity, ECS Trans. 69 (17) (2015) 419–429.
[15] L.W. Wang, S.J. Metcalf, R.E. Critoph, R. Thorpe, Z. Tamainot-Telto, Development of thermal conductive consolidated activated carbon for adsorption refrigeration, Carbon N.Y. 50 (3) (2012) 977–986.
[16] K. Fayazmanesh, C. McCague, M. Bahrami, Consolidated adsorbent containing graphite flakes for heat-driven water sorption cooling systems, Appl. Therm. Eng. 123 (2017) 753–760.
[17] L.W. Wang, Z. Tamainot-Telto, R. Thorpe, R.E. Critoph, S.J. Metcalf, R.Z. Wang, Study of thermal conductivity, permeability, and adsorption performance of consolidated composite activated carbon adsorbent for refrigeration, Renew. Energy 36 (8) (2011) 2062–2066.
[18] K. Wang, J.Y. Wu, R.Z. Wang, L.W. Wang, Effective thermal conductivity of expanded graphite–$CaCl_2$ composite adsorbent for chemical adsorption chillers, Energy Convers. Manage. 47 (13–14) (2006) 1902–1912.
[19] M. Kandula, Effective thermal conductivity of porous packed beds with uniform spherical particles, J. Porous Media 14 (10) (2011) 919–926.
[20] E. Pop, V. Varshney, A.K. Roy, Thermal properties of graphene: fundamentals and applications, MRS Bull. 37 (12) (2012) 1273–1281.